16

Modelling and Control Design of Pitch-Controlled Variable Speed Wind Turbines

Marcelo Gustavo Molina and Pedro Enrique Mercado
CONICET, Instituto de Energía Eléctrica, Universidad Nacional de San Juan
Argentina

1. Introduction

In the past decade, many problems related to energy factors (oil crisis), ecological aspects (climatic change), electric demand (significant growth) and financial/regulatory restrictions of wholesale markets have arisen worldwide. These difficulties, far from finding effective solutions, are continuously increasing, which suggests the need of technological alternatives to assure their solution. Under these circumstances, distributed or dispersed generation (DG) arises as the technological alternative with the ability of giving an effective solution to such difficulties. Distributed generation consists of generating electricity as near as possible of the consumption site, in fact like it was made in the beginnings of the electric industry, but now incorporating the advantages of the modern technology. Here it is consolidated the idea of using clean non-conventional technologies of generation that use renewable energy sources (RESs) that do not cause environmental pollution, such as wind, photovoltaic, wave, hydraulic, and more sophisticated systems based on hydrogen. The main advantages of using RESs as DG systems are the elimination of harmful emissions and inexhaustible resources of the primary energy (Heier, 2006).

Medium to large grid-connected wind turbine generators (WTGs) are particularly becoming today the most important and fastest growing form of electricity generation among the renewable technologies. They attract interest as one of the most cost-effective ways to generate electricity from RESs (Guerrero, et al., 2010). Indeed, this RES technology started in the eighties with a few tens of kW power capacity to date with multi-MW size wind turbines that are being installed. This trend is expected to be increased in the near future, sustained by the cost competitiveness of wind power technology and the development of new power electronics technologies, new circuit topologies and control strategies. These profits include the strong support provided by governments of different countries, as investment subsidies and incentives that impact directly on the commercial acceptance of wind turbine generators.

The growing number of distributed generators, particularly based on wind power systems, brings new challenges to the operation and management of the power distribution system, especially when the intermittent energy source constitutes a significant part of the total system capacity (Rahman, 2003). Under this scenario, the power electronic technology plays an important role in the integration of DG into the electrical grid since the DG system is subject to requirements related not only to the RES itself but also to its effects on the power

system operation. The use of power electronic converters enables wind turbines to operate at variable (or adjustable) speed, and thus permits to provide more effective power capture than the fixed speed counterparts (Timbus et al., 2009). In fact, variable speed wind turbines have demonstrated to capture 8-15% more energy than constant speed machines. In variable speed operation, a control system designed to extract maximum power from the wind turbine and to provide constant grid voltage and frequency is required. As well as becoming larger, wind turbine designs were progressing from fixed speed, stall-controlled and with drive trains with gear boxes to become pitch controlled, variable speed and with or without gearboxes.

Among variable speed wind turbine generators, direct-in-line systems and doubly-fed induction generator (DFIG) systems have increasingly drawn more interests to wind turbine manufactures due to their advantages over other variable speed wind turbines and currently have the most significant potential of growth. Direct-in-line systems consists of a direct-driven (without gearbox) permanent magnet synchronous generator (PMSG) grid-connected via a full-scale power converter, while DFIG systems are built with a common induction generator with slip ring and a partial-scale converter connected to the rotor windings. Both modern pitch-controlled variable speed wind turbines technologies are emerging as the preferred technologies and have become the dominating type of yearly installed wind turbines in recent years.

2. Wind energy development

Worldwide, the development of wind energy is experiencing dramatic growth. During the last decade, the installed wind energy capacity has grown rapidly. According to the Global Wind Energy Council (GWEC), 15 197 MW of wind power capacity have been installed in 2006 in more than 40 countries, an increase of 32% over 2005. The installation of the total global wind energy capacity was increased to 74 223 MW by the end of 2006 from 59 091 MW of 2005. In terms of economic value, the wind energy sector has presently become one of the important players in the energy markets, with the total value of new generating equipment installed in 2006 reaching $ 23 billion (approximately € 18 billion) (Global wind energy council, 2006).

Europe continues to be the world major player in the installation of wind power systems. In 2006, the country having the highest total installed capacity was Germany with 20 621 MW. Spain and the United States are in second and third place, each with a little more than 11 603 MW installed. India is in fourth place, and Denmark ranks fifth. Asia experienced the strongest increase in installed capacity outside of Europe, with an addition of 3679 MW, taking the total capacity over 10 600 MW, about half that of Germany. The Chinese market was increased by the country's new Renewable Energy Law. China has more than doubled its total installed capacity by installing 1347 MW of wind energy in 2006, a 70% increase over 2005. This brings China up to 2604 MW of capacity, making it the sixth largest market worldwide. It is expected that more than 40 GW will be installed by 2020; this may become China the third major power supply by that year. Growth in African and Middle Eastern market also picked up in 2006, with 172MW of new installed capacity, mainly in Egypt, Morocco, and Iran, bringing the total up to 441 MW, a 63% growth (Blaabjerg & Chen, 2006).

The European Wind Energy Association (EWEA) has set a target to satisfy 23% European electricity needs with wind by 2030. The exponential growth of the wind industry reflects the increasing demand for clean, safe and domestic energy and can be attributed to

government policies associated with the environmental concerns, and research and development of innovative cost-reducing technologies.
The large scale development of wind power results in the wind turbines/farms becoming a significant part of the generation capacity in some area, which requires that the power system treats the wind turbines/farms like a power source, not only an energy source. The wind power penetration would result in variations of load flows in the interconnected systems, as well as re-dispatch of conventional power plants, which may cause a reduction of reserve power capacity (Slootweg & Kling, 2003). Some actions become necessary to accommodate large scale wind power penetration. For example, the electric grid may need an expansion for bulk electricity transmission from offshore wind farms to load centers, and it may require reinforcement of existing power lines or construction of new power lines, installation of Flexible AC Transmission system (FACTs) devices, etc.

3. Modern wind power systems

The discovery of electricity generated using wind power dates back to the end of last century and has encountered many ups and downs in its more than 100 year history. In the beginning, the primary motivation for essentially all the researches on wind power generation was to reinforce the mechanization of agriculture through locally-made electricity generation. Nevertheless, with the electrification of industrialized countries, the role of wind power drastically reduced, as it could not compete with the fossil fuel-fired power stations. This conventional generation showed to be by far more competitive in providing electric power on a large scale than any other renewable one.
Lack of fossil fuels during World War I and soon afterward during World War II created a consciousness of the great dependence on fossil fuels and gave a renewed attention to renewable energies and particularly to wind power. Although this concern did not extend long. The prices for electricity generated via wind power were still not competitive and politically nuclear power gained more attention and hence more research and development funds. It took two oil crises in the 1970s with supply problems and price fluctuations on fossil fuels before wind power once again was placed on the agenda. And they were these issues confronting many countries in the seventies which started a new stage for wind power and motivated the development of a global industry which today is characterized by relatively few but very large wind turbine manufacturers.
The beginning of modern wind turbine development was in 1957, marked by the Danish engineer Johannes Juul and his pioneer work at a power utility (SEAS at Gedser coast in the Southern part of Denmark). His R&D effort formed the basis for the design of a modern AC wind turbine – the well-known Gedser machine which was successfully installed in 1959. With its 200kW capacity, the Gedser wind turbine was the largest of its kind in the world at that time and it was in operation for 11 years without maintenance. The robust Gedser wind turbine was a technological innovation as it became the hall mark of modern design of wind turbines with three wings, tip brakes, self-regulating and an asynchronous motor as generator. Foreign engineers named the Gedser wind turbine as 'The Danish Concept'.
Since then, the main aerodynamic concept has been this horizontal axis, three-bladed, upwind wind turbine connected to a three-phase electric grid, although many other different concepts have been developed and tested over the world with dissimilar results. An example of other concepts is the vertical axis wind turbine design by Darrieus, which provides a different mix of design tradeoffs from the conventional horizontal-axis wind

turbine. The vertical orientation accepts wind from any direction with no need for adjustments, and the heavy generator and gearbox equipment can rest on the ground instead of on top of the tower.

The aim of wind turbine systems development is to continuously increase output power, as depicted in Fig. 1. Since the rated output power of production-type units reached 200 kW various decades ago, by 1999 the average output power of new installations climbed to 600 kW. Today, the manufactured turbines for onshore applications are specified to deliver 2-3 MW output power. In this sense, the world's first wind park with novel "multi-mega power class" 7 MW wind turbines was manufactured by the German wind turbine producer Enercon (11 E-126 units) and put into partial operation in Estinnes, Belgium, in 2010 (to be completed by July 2012). The key objective of this 77 MW pilot project is to introduce a new power class of large-scale wind energy converters (7 MW WECs) into the market with potential to significantly contribute to higher market penetration levels for wind electricity, especially in Europe. On the other hand, sea-based wind farms are likely to mean bigger turbines than on land, with models that produce up to three times the power of standard on-shore models. Series production of offshore wind turbines can reach to date up to 5 MW or more, being the largest onshore wind turbine presently under development a 10 MW unit. At least four companies are working on the development of this "giant power class" 10 MW turbine for sea-based applications, namely American Superconductors (U.S.), Wind Power (U.K.), Clipper Windpower (U.K.) and Sway (Norway). Even more, it is likely that in the near future, power rating of wind turbines will increase further, especially for large-scale offshore floating wind turbine applications.

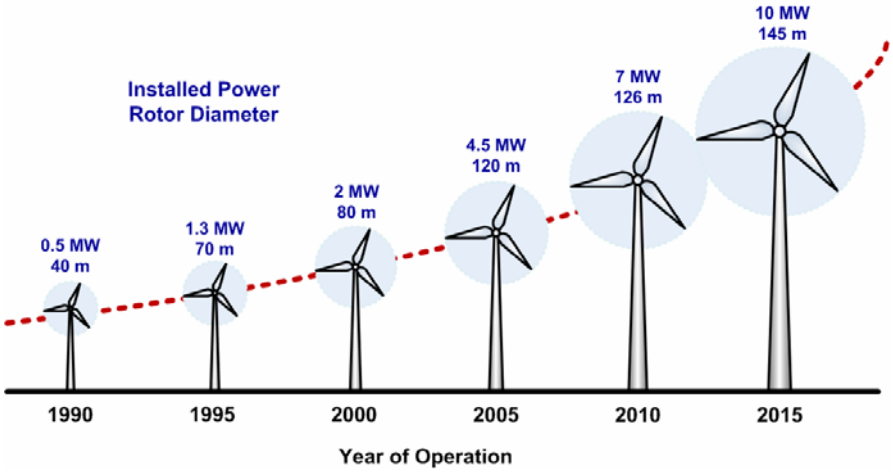

Fig. 1. Size evolution of wind turbines over time

4. Wind energy conversion

A wind turbine is a rotary engine that captures power from a fluid flow (the wind) using aerodynamically designed blades and convert it into useful mechanical power. The available power depends on the wind speed but it is important to be able to control and limit the power at higher wind speeds so as to avoid the damage of the unit. The power limitation

may be done by some of the three following methods, namely stall control (the blade position is fixed but stall of the wind appears along the blade at higher wind speed), active stall (the blade angle is adjusted in order to create stall along the blades) or pitch control (the blades are turned out of the wind at higher wind speed). Essentially, three types of typical wind generator systems are the most widely spread. The first type is a constant-speed wind turbine system with a standard squirrel-cage induction generator (SCIG) directly connected to the grid. The second type is a variable speed wind turbine system with a doubly fed induction generator (DFIG). The power electronic converter feeding the rotor winding has a power rating of approximately up to 30% of the rated power; the stator winding of the DFIG is directly connected to the grid. The third type is a variable speed wind turbine with full-rated power electronic conversion system and a synchronous generator or a SCIG. A multi-stage gearbox is usually used with the first two types of generators. Synchronous generators, including permanent magnet synchronous generator (PMSG), may be direct driven though a low-ratio gear box system; one or two stage gearbox, becomes an interesting option. Fig. 2 summarized the major parts included in the mechanical and electrical power conversion of a typical wind turbine system (Chen & Blaabjerg, 2009).

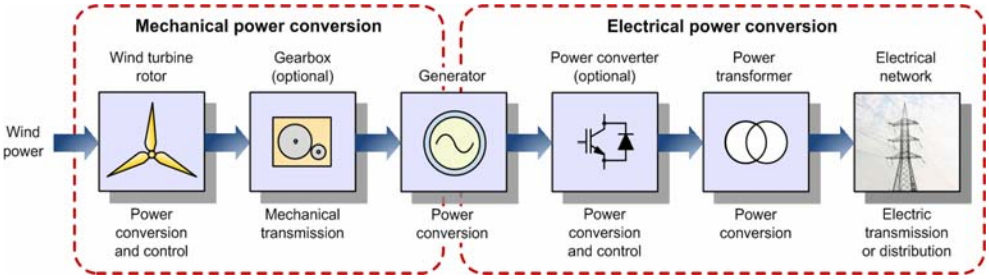

Fig. 2. General description of a wind turbine system

The appropriate voltage level is related to the generated power level. A modern wind turbine is often equipped with a transformer stepping up the generator terminal voltage, usually a voltage below 1 kV (E.g. 575 or 690 V), to a medium voltage around 20-30 kV, for the local electrical connection within a wind farm (distribution level). If the wind farm is large and the distance to the electrical grid is long, a transformer may be used to further step up the medium voltage in the wind farm to a high voltage at transmission level. For instance, for large onshore wind farms at hundreds of MWs, high voltage overhead lines above 100 kV are usually employed. For offshore wind farms with a long distance transmission to an onshore grid, the power generated is transferred by submarine cables buried in the sea bed. The cables between the turbines are linked to a transformer substation, which, at most cases, is placed offshore near the wind farm due to the long distance to shore (more than 5 km from the shore).

Basically, a wind energy conversion system consists of a turbine tower which carries the nacelle, and the wind turbine rotor, consisting of rotor blades and hub. Most modern wind turbines are horizontal-axis wind turbines (HAWTs) with three rotor blades usually placed upwind of the tower and the nacelle, as illustrated in Fig. 3. On the outside, the nacelle is usually equipped with anemometers and a wind vane to measure the wind speed and direction, as well as with aviation lights. The nacelle contains the key components of the wind turbine, i.e. the gearbox, mechanical brake, electrical generator, control systems, yaw

drive, etc. The wind turbines are not only installed dispersedly on land, but also combined as wind farms (or parks) with capacities of hundreds MWs which are comparable with modern power generator units. Consequently, their performance could significantly affect power system operation and control (Hansen, et al. 2004).

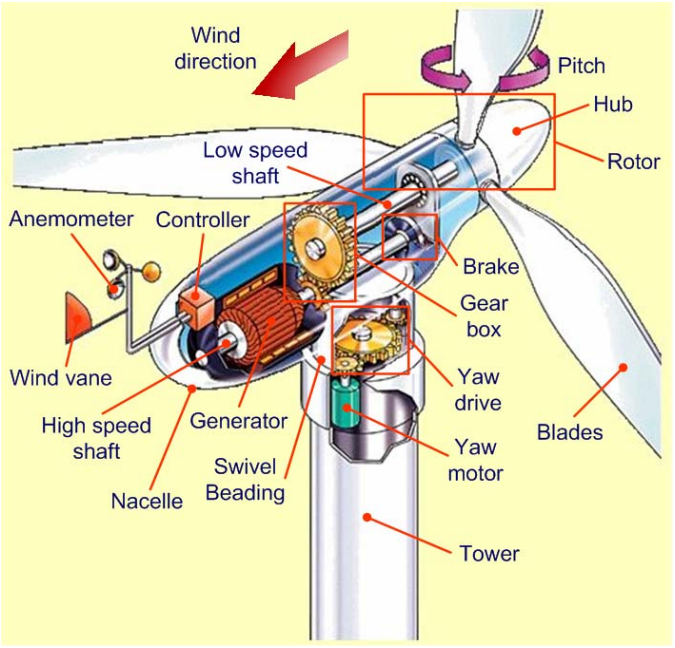

Fig. 3. Major components of a typical horizontal axis, three-bladed, upwind wind turbine

5. Wind turbine concepts

Wind turbines can either be designed to operate at fixed speed (actually within a speed range about 1%) or at variable speed. Many low-power wind turbines built to-date were constructed according to the so-called "Danish concept" that was very popular in the eighties, in which wind energy is transformed into electrical energy using a simple squirrel-cage induction machine directly connected to a three-phase power grid (Qiao et al., 2007). The rotor of the wind turbine is coupled to the generator shaft with a fixed-ratio gearbox. At any given operating point, this turbine has to be operated basically at constant speed. On the other hand, modern high-power wind turbines in the 2-10 MW range are mainly based on variable speed operation with blade pitch angle control obtained mainly by means of power electronic equipment, although variable generator rotor resistance can also be used. These wind turbines can be mostly developed using either a direct-in-line system built with a direct-driven (without gearbox) PMSG grid-connected via a full-scale power converter, or a doubly-fed induction generator (DFIG) system that consists of a DFIG with a partial-scale power converter connected to the rotor windings. Based on these concepts, the most commonly applied wind turbine designs can be classified into four wind turbine concepts, as described below.

5.1 Type A – Fixed speed wind turbine

This topology corresponds to the constant or fixed speed controlled wind turbine, with asynchronous squirrel cage induction generator (SCIG) directly connected to the electric grid using a step up power transformer, as depicted in Fig. 4. Since the squirrel cage induction generator always draws reactive power from the AC network, this concept requires a reactive power compensator, such as a capacitor bank, in order to reduce or even eliminate the reactive power demand from these turbine generators to the grid. It is typically achieved by continuously switching capacitor banks (5-25 steps) according to the active power generated. A smoother grid connection occurs by including a soft starter. Regardless the power control principle in a fixed speed machine, the wind fluctuations are converted into mechanical fluctuations and further into electrical power fluctuations. These can cause voltage fluctuations at the point of common coupling (PCC) of the wind turbine to the electric grid when the network is weak. Because of these voltage fluctuations, the fixed speed wind turbine draws fluctuating reactive power from the utility grid (in the case of no use of capacitor bank), which increases both the voltage fluctuations and the line losses. Fixed speed systems have the advantage of simplicity and low cost; however, the main drawbacks of this concept include the inability of supporting speed control, the requirement of a stiff grid (fixed voltage and frequency), and the necessity of a robust mechanical structure in order to support the high mechanical stress caused by wind gusts.

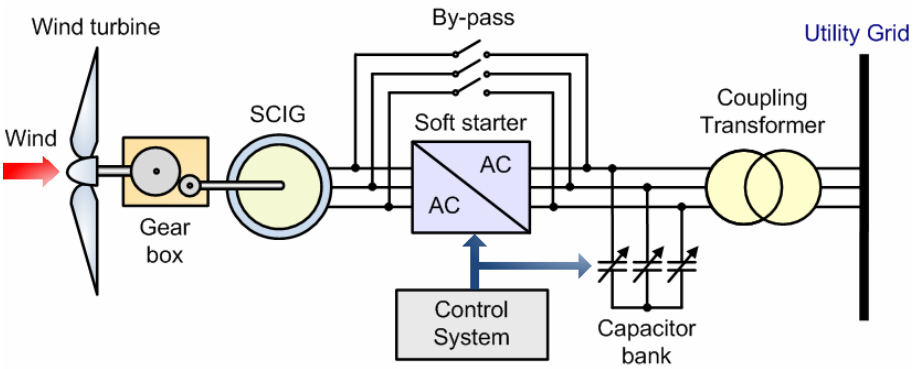

Fig. 4. Type A wind turbine concept: Fixed speed wind turbine directly connected to the electric grid via a squirrel cage induction generator

5.2 Type B – Partial variable speed wind turbine with variable rotor resistance

This topology corresponds to the partial variable speed controlled wind turbine with variable generator rotor resistance, aka OptiSlip by the Danish manufacturer Vestas™ Wind Systems (Krüger & Andresen, 2001), as presented in Fig. 5. It uses a wound rotor induction generator (WRIG) and has been used since the mid-nineties. In this case, the configuration is analogous to the type A wind turbine concept, with a generator directly connected to the electric grid. However, the rotor windings of the generator are connected in series with a controlled resistance, whose size defines the range of the variable speed (typically 0-10% above the synchronous speed). A capacitor bank performs reactive power compensation and a smoother grid connection is obtained by including a soft starter. The distinctive feature of this concept is that it has a variable additional rotor resistance, which is changed by an

optical controlled converter mounted on the rotor shaft. Thus the rotor resistance is controllable, but eliminates the need for costly slip rings, which needs brushes and maintenance, through the optically coupling patented system. By varying the rotor resistance, the slip and thus the power output of the wind turbine can be controlled. The dynamic speed control range varies with the size of the variable rotor resistance and commonly reaches up to 10% above the synchronous speed. The energy coming from the external power conversion unit is dumped as heat loss.

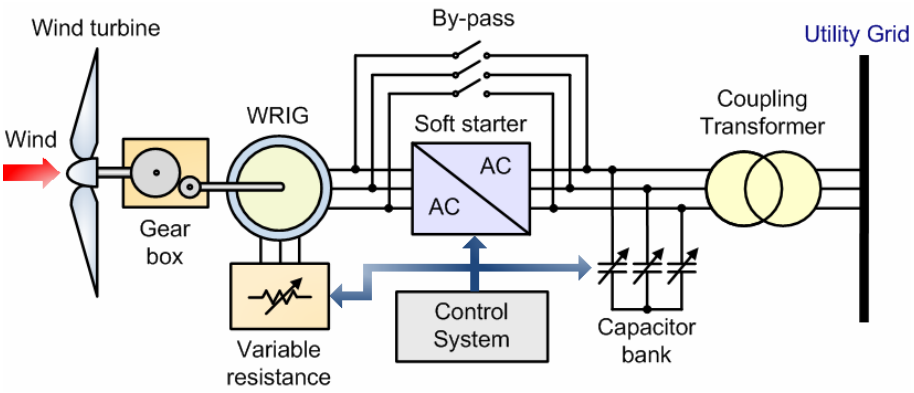

Fig. 5. Type B wind turbine concept: Partial variable speed wind turbine directly connected to the electric grid via a wound rotor induction generator with variable rotor resistance

5.2 Type C – Variable speed wind turbine with partial-scale power converter

This concept, aka doubly-fed induction generator (DFIG), corresponds to a variable speed controlled wind turbine with a wound rotor induction generator (WRIG) and a partial-scale power converter (rated approximately at 30% of nominal generated power) on the rotor circuit (Muller et al, 2002). The use of power electronic converters enables wind turbines to operate at variable (or adjustable) speed, and thus permits to provide more effective power capture than the fixed-speed counterparts. In addition, other significant advantages using variable speed systems include a decrease in mechanical loss, which makes possible lighter mechanical designs, and a more controllable power output (less dependent on wind variations), cost-effectiveness, simple pitch control, improved power quality and system efficiency, reduced acoustic noise, and island-operation capability. As shown in Fig. 6, the rotor stator is directly connected to the electric grid, while a partial-scale power converter controls the rotor frequency and consequently the rotor speed. The partial-scale power converter is composed of a back-to-back four-quadrant AC/DC/AC converter design based on insulated gate bipolar transistors (IGBTs), whose power rating defines the speed range (typically around ±30% of the synchronous speed). Moreover, this converter allows controlling the reactive power compensation and a smooth grid connection. The control range of the rotor speed is larger than that of the type C concept (Vestas´s OptiSlip). Even more, it captures the energy which is burned off in the controllable rotor resistance of the type C concept; this allows enhancing the efficiency of the overall system. The smaller power converter makes this concept attractive from an economical point of view. However, its main drawbacks are the use of slip rings, which needs brushes and maintenance, and the complex protection schemes in the case of grid faults.

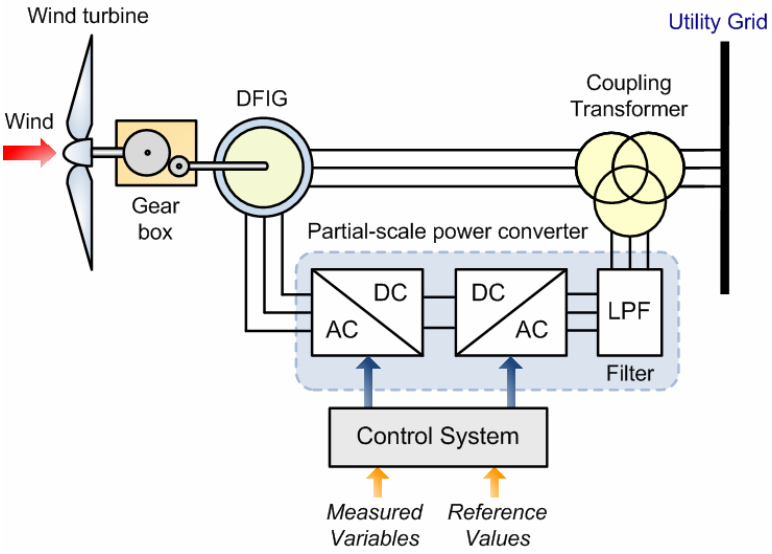

Fig. 6. Type C wind turbine concept: Variable speed wind turbine directly connected to the electric grid via a doubly-fed induction generator controlled with a partial-scale power converter

5.3 Type D – Direct-in-line variable speed wind turbine with full-scale power converter

This configuration corresponds to the direct-in-line full variable speed controlled wind turbine, with the generator connected to the electric grid through a full-scale power converter. A synchronous generator is used to produce variable frequency AC power. The power converter connected in series (or in-line) with the wind turbine generator transforms this variable frequency AC power into fixed-frequency AC power. This power converter also allows controlling the reactive power compensation locally generated, and a smooth grid connection for the entire speed range. The generator can be electrically excited (wound rotor synchronous generator, WRSG) or permanent magnet excited type (permanent magnet synchronous generator, PMSG). Recently, due to the development in power electronics technology, the squirrel-cage induction generator (SCIG) has also started to be used for this concept. As illustrated in Fig. 7, the generator stator is connected to the grid through a full-scale power converter, which is composed of a back-to-back four-quadrant AC/DC/AC converter design based on insulated gate bipolar transistors (IGBTs). Some full variable speed wind turbine systems have no gearbox (shown in dotted lines in Fig. 7) and use a direct driven multi-pole generator.

Direct-in-line variable speed wind turbines have several drawbacks respect to the former variable speed DFIG concepts, which mainly include the power converter and output filter ratings at about 1 p.u. of the total system power. This feature reduces the efficiency of the overall system and therefore results in a more expensive device. However, as the full scale power converter decouples entirely the wind turbine generator from the utility grid, grid codes such as fault ride through and grid support are easier to be accomplished, as required from modern applications. In addition, since a direct-in-line system can operate at low speeds, the gearbox can be omitted (direct-driven). Consequently, a gearless construction

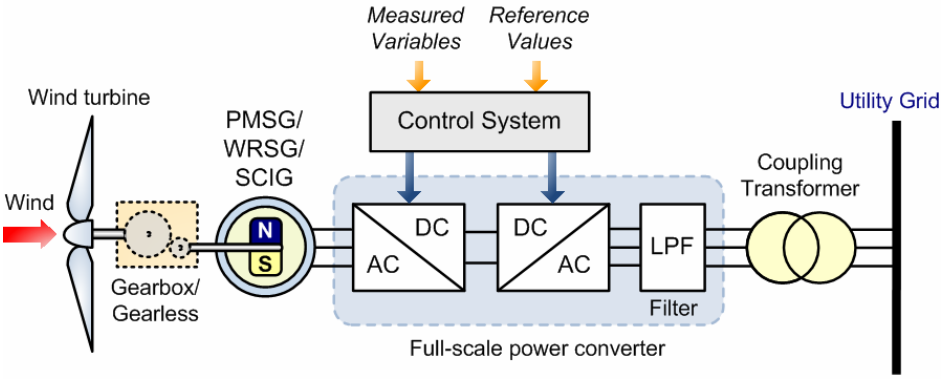

Fig. 7. Type D wind turbine concept: Direct-in-line variable speed wind turbine connected to the electric grid through a full-scale power converter

represents an efficient and robust solution that is beneficial, especially for offshore applications, where low maintenance requirements are essential. Moreover, using a permanent magnet synchronous generator, the DC excitation system is eliminated and allows reducing weight, losses, costs, and maintenance requirements (no slip rings are required). Even more, due to the intensified grid codes around the world, direct-driven PMSG wind turbine systems could be favored in the future compared to DFIG wind turbine concepts (Li et al., 2009).

6. Modelling of a direct-driven PMSG wind turbine system

This section presents the mathematical model for each component of the individual direct-in-line wind turbine system, including the wind turbine, the mechanical shaft system, the generator and the power electronic interface with the electric utility grid. The modeling approach of the proposed wind turbine system is based on the general structure presented in Fig. 7. The wind turbine generator considered in this work employs a direct-driven (without gearbox) PMSG directly coupled to the wind turbine and connected to the electric grid through the power conditioning system (PCS). The stator windings of the PMSG are directly connected to the PCS composed of a full-scale power converter built using a back-to-back AC/DC/AC power converter topology which includes a three-phase rectifier bridge (AC/DC conversion), a DC/DC converter and a grid-side converter with an intermediate DC link (DC/AC conversion) (Blaabjerg et al., 2004).

6.1 Wind turbine

The wind turbine employed in this work is a classic three-bladed horizontal-axis (main shaft) wind turbine design. This turbine was implemented and characterized using a laboratory-scale 0.5 kW rated power (at 12.5 m/s) prototype. Since the turbine corresponds to a small-scale one, no active blade pitch control is implemented and instead a self-regulation (passive stall control) through blades twisting is employed.

The proposed model is based on the steady-state aerodynamic power characteristics of the wind turbine. The output mechanical power available from a variable speed wind turbine can be expressed through the following algebraic relation (Freris, 1990; Ackermann, 2005).

$$P_m = \frac{1}{2}\rho\, A\, v^3\, C_p(\lambda,\beta)\ , \tag{1}$$

where:

ρ: air density (typically 1.225 kg/m^3 at sea level with standard conditions, i.e. temperature of 15 °C and atmospheric pressure of 101.325 kPa)

A: area swept by the rotor blades

v: wind speed

C_p: so-called power coefficient (aka coefficient of performance) of the wind turbine.

The power coefficient C_p is a nonlinear function of the blade pitch angle β and the tip-speed ratio λ as given by equation (2).

$$\lambda = \left(\frac{R\,\omega_m}{v}\right), \tag{2}$$

with:

R: radius of the turbine blades

ω_m: angular speed of the turbine rotor

As can be derived from equation (1), the power coefficient C_p is given in terms of the blade pitch angle β and the tip-speed ratio λ. Since the proposed wind turbine can operate over a wide range of rotor speeds, the assumption of linear torque versus speed characteristic (at a given wind speed and blade pitch angle) cannot be used and thus the aerodynamic system results very complex to be analytically determined. Consequently, numerical approximations have been developed in order to calculate the mechanical power characteristic of the wind turbine and a bi-dimensional characteristic function of C_p has been used (Raiambal & Chellamuthu, 2002) and validated in the laboratory.

$$C_p(\lambda,\beta) = \frac{1}{2}\left(\frac{98}{\lambda_i} - 0.4\beta - 5\right)\exp\left(\frac{-16.5}{\lambda_i}\right), \tag{3}$$

with:

$$\lambda_i = \left[\frac{1}{(\lambda + 0.089)} - \frac{0.035}{\left(\beta^3 + 1\right)}\right]^{-1} \tag{4}$$

The characteristic function C_p vs. λ, for various values of the pitch angle β, is shown in Fig. 8. The maximum value of C_p, that is C_{pmax}=0.47, is achieved for β=0° and for λ=6.75. This particular value λ_{opt} results in the point of optimal efficiency where the maximum power is captured from wind by the wind turbine.

Fig. 9 illustrates the mechanical power versus the rotating speed of the proposed wind power system with no blade pitch angle control (β=0°) at various wind speeds. As can be derived, there exists a good agreement between the results obtained with both scaled laboratory prototype and the corresponding model. It can be also observed that, for each wind speed, there exists a specific point in the wind generator power characteristic, aka maximum power point (MPP), where the output power is maximized. Thus, the control of the wind turbine power results in a variable speed operation aiming at tracking the MPP for

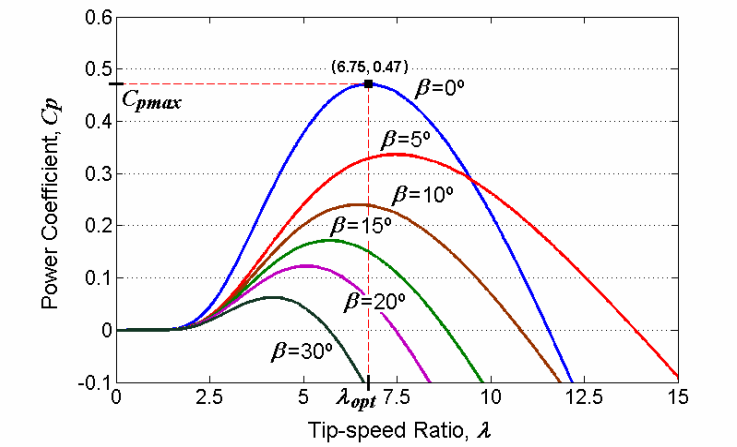

Fig. 8. Characteristics function C_p vs. λ, at various pitch angle values for the studied wind turbine generator

the particular operating conditions such that the maximum power can be continuously extracted from the wind (MPP tracking control or MPPT).

6.2 Mechanical shaft system

The mechanical shaft system of the WTG can be usually represented either by a two-mass system or by a single-mass lumped-parameter system. In the case of direct-in-line variable speed wind power systems, because the wind turbine is connected to the electric grid through a full-scale converter, the shaft properties are hardly reflected at the grid connection due to the decoupling effect of the power conditioning system. In this way, the turbine rotor

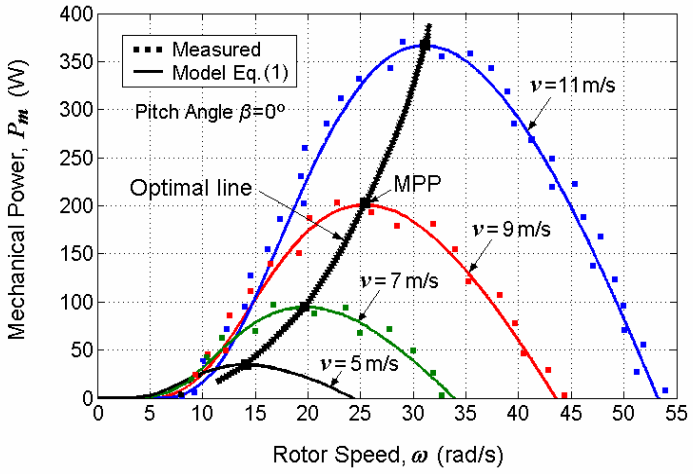

Fig. 9. Mechanical power versus rotor speed curves measurements and simulations at various wind speeds for the studied wind turbine generator

is modeled as a lumped mass and the shaft dynamics is neglected. Even more, since multi-pole PMSGs have increasingly been used in variable speed generators, in such a way that they can operate at low speeds, the gearbox can be omitted. Consequently, a direct-driven (gearless) construction represents an efficient and robust solution that is beneficial.
The wind turbine rotor dynamics can be modeled as:

$$T_e = T_l + B_f \omega_m + J_c \frac{d\omega_m}{dt} \tag{5}$$

where:
T_e: electromagnetic torque of the electric machine
T_l: load torque
B_f: viscous friction coefficient
J_c: combined inertia moment of the WTG rotor and PMSG
ω_m: rotor mechanical speed, which is related to the rotor angular speed of the electric machine ω_s, through:

$$\omega_m = \frac{\omega_s}{p_p} \tag{6}$$

with p_p being the number of pole-pairs of the generator.

6.3 Permanent magnet synchronous generator

The permanent magnet synchronous machine can be electrically described in steady-state using a simple equivalent circuit with an armature equation including back electromotive forces (emfs). This model assumes that saturation is neglected, the induced emfs are sinusoidal, the Eddy currents and hysteresis losses are negligible, and that there are no field current dynamics. In this way, voltage equations for the PMSG are given by:

$$\begin{bmatrix} u_{am} \\ u_{bm} \\ u_{cm} \end{bmatrix} - \begin{bmatrix} u_a \\ u_b \\ u_c \end{bmatrix} = (\mathrm{R_m} + s\mathrm{L}) \begin{bmatrix} i_{am} \\ i_{bm} \\ i_{cm} \end{bmatrix} \tag{7}$$

where:

$$\mathrm{R_m} = \begin{bmatrix} R_m & 0 & 0 \\ 0 & R_m & 0 \\ 0 & 0 & R_m \end{bmatrix}, \qquad \mathrm{L} = \begin{bmatrix} L_{aa} & L_{ab} & L_{ac} \\ L_{ab} & L_{bb} & L_{bc} \\ L_{ac} & L_{bc} & L_{cc} \end{bmatrix}, \tag{8}$$

being:
s: Laplace variable, with $s = d/dt$ for t > 0 (Heaviside operator p also used)
u_{im} (i=a,b,c): stator phase voltages in a-b-c coordinates
u_i: back emfs in a-b-c coordinates
i_{im}: stator currents in a-b-c coordinates
L_{ij}: stator winding inductances, including self and mutual ones (combinations of i and j=a, b, c). It is considered symmetry for mutual inductances, so that L_{ij}=L_{ji}

The terminal voltages applied from the machine-side converter to the stator, u_{im} and the back emfs, u_i are balanced three-phase voltages, being the later defined as follows:

$$u_i = \omega_s \Psi_{mi} \tag{9}$$

with:

Ψ_{mi}: permanent-magnet flux linkage in *a-b-c* coordinates

Since there is no functional equation for instantaneous reactive power in the *a-b-c* reference frame, it is useful to apply a transformation to the synchronous-rotating orthogonal *d-q* set aligned with the rotor flux, to equations (7) and (8) in order to analyze the electric machine. This is performed by applying Park's transformation and defining the *q*-axis to be always coincident with the instantaneous stator magneto-motive forces (mmfs), which rotate at the same angular speed as that of the rotor (yielding u_q equals $|u|$, while u_d is null). This is beneficial because any AC signals that spins at ω_s become DC quantities in the rotor *d-q* frame. Then, by neglecting the zero sequence components, equations (10) and (11) are derived.

$$\begin{bmatrix} u_{dm} \\ u_{qm} \end{bmatrix} - \begin{bmatrix} u_d \\ u_q \end{bmatrix} = \left(\mathrm{R_m} + s\mathrm{L'_s}\right) \begin{bmatrix} i_{dm} \\ i_{qm} \end{bmatrix} + \begin{bmatrix} -\omega_s & 0 \\ 0 & \omega_s \end{bmatrix} \mathrm{L'_s} \begin{bmatrix} i_{qm} \\ i_{dm} \end{bmatrix} \tag{10}$$

where:

$$\mathrm{R_m} = \begin{bmatrix} R_m & 0 \\ 0 & R_m \end{bmatrix}, \qquad \mathrm{L'_s} = \begin{bmatrix} L_d & 0 \\ 0 & L_q \end{bmatrix}, \qquad u_d = \omega_s \Psi_{qm}, \qquad u_q = \omega_s \Psi_{dm} \tag{11}$$

Flux Linkages in the *d-q* frame can be expressed in terms of the stator currents, inductances, and the flux linkage due to the permanent magnets of the rotor linking the stator, Ψ_m as:

$$\Psi_{dm} = L_d i_{dm} + \Psi_m \tag{12}$$

$$\Psi_{qm} = L_q i_{qm} \tag{13}$$

By rewriting equation (10), the following state equation is obtained:

$$s \begin{bmatrix} i_{dm} \\ i_{qm} \end{bmatrix} = \begin{bmatrix} \dfrac{-R_m}{L_d} & \omega_s \\ -\omega_s & \dfrac{-R_m}{L_q} \end{bmatrix} \begin{bmatrix} i_{dm} \\ i_{qm} \end{bmatrix} + \begin{bmatrix} \dfrac{u_{dm}}{L_d} \\ \dfrac{u_{qm} - |u|}{L_q} \end{bmatrix} \tag{14}$$

being $|u| = \omega_s \Psi_m$

In the rotor *d-q* frame, the active and reactive power flows are calculated as follows:

$$p = \frac{3}{2}(v_{dm} i_{dm} + v_{qm} i_{qm}) \tag{15}$$

$$q = \frac{3}{2}(v_{dm} i_{qm} - v_{qm} i_{dm}) \tag{16}$$

The developed electromagnetic torque of the electric machine takes the following convenient form:

$$T_e = \frac{3}{2} p_p \left[\psi_m i_{qm} + (L_d - L_q)\, i_{dm} i_{qm} \right] \tag{17}$$

For a non-salient-pole machine, as the considered in this analysis, the stator winding direct and quadrature inductances L_d and L_q, are approximately equal. Indeed this application uses a surface mount permanent magnet synchronous machine (SPMSM) which has zero saliency. This means that the direct-axis current i_{dm} does not contribute to the electrical torque T_e. The key concept is to keep null the direct current i_{dm} using appropriate transformation synchronization in order to obtain maximal torque with minimum current i_{qm} (Li et al., 2009).

6.4 Power conditioning system

The power conditioning system (PCS) used for connecting renewable energy sources to the distribution utility grid requires generation of high quality electric power, being at the same time flexible, efficient and reliable (Mohan et al., 1995). Fig. 10 shows the detailed model of a modern direct-in-line variable-speed direct-driven PMSG wind turbine connected to the utility distribution grid, which is composed of a back-to-back AC/DC/AC power converter that fulfills all the requirements mentioned above (Carrasco et al., 2006).

Since the permanent magnet synchronous generator produces an output voltage with variable amplitude and frequency, additional conditioning is required to meet the amplitude and frequency requirements of the roughly stiff utility grid. A three-phase uncontrolled full-wave rectifier bridge is proposed here for performing the AC/DC conversion. This device has the benefit of being simple, robust, cheap, and needs no control system. On the other hand, a three-phase three-level DC/AC voltage source inverter (VSI) using IGBTs is employed for connecting to the grid. As the power rating of the inverter is lesser than a few MWs, the output voltage control of the VSI can be achieved through pulse width modulation (PWM) techniques. This power inverter topology is proposed above other ones because generates a more sinusoidal output voltage waveform than conventional structures without increasing the switching frequency. In this way, the harmonic performance of the inverter is improved, also obtaining better efficiency and reliability respect to the conventional two-level inverter topology. The connection to the utility grid is made through a step-up transformer and a low pass filter in order to reduce the perturbation on the distribution system from high-frequency switching harmonics generated by the PWM control.

As the VSI needs a fixed DC link in order to allow a decoupled control of both active and reactive power exchange with the electric grid, an interface in the DC side of the VSI is required. For this purpose, an intermediate DC/DC converter in a boost topology is used, linking the output of the full-wave rectifier bridge to the DC bus of the power inverter. Only one power switching device is used in the DC/DC converter, resulting in a low cost and simple control. This two-stage AC/DC energy conversion system offers an additional degree of freedom in the operation of the system when compared with conventional one-stage configurations, permitting to pursue various control objectives simultaneously with the WTG system operation.

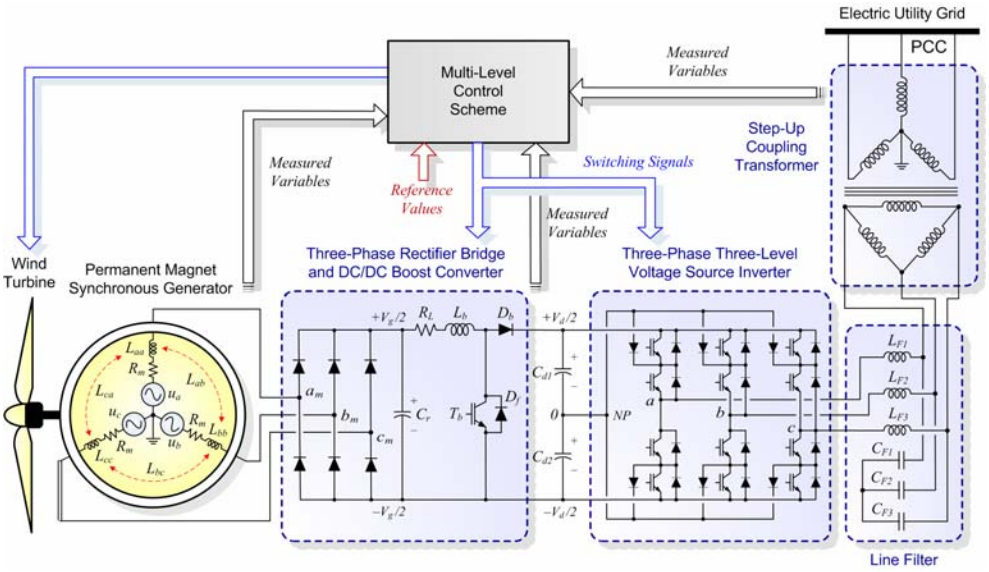

Fig. 10. Detailed model of a modern variable-speed direct-driven PMSG wind turbine connected to the utility distribution grid

6.4.1 DC/DC Converter

The standard unidirectional topology of the DC/DC boost converter (also known as step-up converter or chopper) consist of a switching-mode power device containing basically two semiconductor switches (a rectifier diode and a power transistor with its corresponding anti-parallel diode) and two energy storage devices (an inductor and a smoothing capacitor) for producing an output DC voltage at a level greater than its input dc voltage. This converter acts as an interface between the full-wave rectifier bridge and the VSI, by employing pulse-width modulation (PWM) control techniques.

Operation of the DC/DC converter in the continuous (current) conduction mode (CCM), i.e. the current flowing continuously in the inductor during the entire switching cycle, makes simple the development of the state-space model because only two switch states are possible during a switching cycle, namely, (*i*) the power switch T_b is *on* and the diode D_b is *off*; or (*ii*) T_b is *off* and D_b is *on*.

In steady-state CCM operation and neglecting parasitic components, the state-space equation that describes the dynamics of the DC/DC boost converter is given by equation (18) (Molina & Mercado, 2008).

$$\begin{bmatrix} sI_L \\ sV_d \end{bmatrix} = \begin{bmatrix} 0 & -\dfrac{1-S_{dc}}{L} \\ \dfrac{1-S_{dc}}{C} & 0 \end{bmatrix} \begin{bmatrix} I_L \\ V_d \end{bmatrix} + \begin{bmatrix} \dfrac{1}{L} & 0 \\ 0 & -\dfrac{1}{C} \end{bmatrix} \begin{bmatrix} V_g \\ I_d \end{bmatrix}, \tag{18}$$

where:

I_L: chopper input current (inductor current).

V_g: chopper input voltage, the same as the three-phase rectifier output voltage.
V_d: chopper output voltage, coinciding with the inverter DC bus voltage.
i_d: chopper output current.
S_{dc}: switching function of the boost DC/DC converter.
The switching function S_{dc} of the power converter is a two-levelled waveform characterizing the signal that drives the power switch T_b of the DC/DC boost converter, defined as follows:

$$S_{dc} = \begin{cases} 0, \text{ for the switch } T_b \textit{ off} \\ 1, \text{ for the switch } T_b \textit{ on} \end{cases} \tag{19}$$

If the switching frequency of the power switches is significantly higher than the natural frequencies of the DC/DC converter, this discontinuous model can be approximated by a continuous state-space averaged (SSA) model, where a new variable D is introduced. In the [0, 1] interval, D is a continuous function and represents the modulation index of the DC/DC converter, defined as the ratio of time during which the power switch T_b is turned-on to the period of one complete switching cycle, T_s. This variable is used for replacing the switching function in equation (18), yielding the following SSA expression:

$$\begin{bmatrix} sI_L \\ sV_d \end{bmatrix} = \begin{bmatrix} 0 & -\frac{1-D}{L} \\ -\frac{1-D}{C} & 0 \end{bmatrix} \begin{bmatrix} I_L \\ V_d \end{bmatrix} + \begin{bmatrix} \frac{1}{L} & 0 \\ 0 & -\frac{1}{C} \end{bmatrix} \begin{bmatrix} V_g \\ I_d \end{bmatrix} \tag{20}$$

Since, in steady-state conditions the inductor current variation during both, on and off times of T_b are essentially equal, so there is not net change of the inductor current from cycle to cycle, and assuming a constant Dc output voltage of the boost converter, the steady-state input-to-output voltage conversion relationship of the boost converter is easily derived from equation (20) by setting the inductor current derivative at zero, yielding equation (21):

$$V_d = \frac{V_g}{(1-D)} \tag{21}$$

In the same way, the relationship between the average inductor current I_L and the DC/DC converter output current I_d in the CCM can be derived, as follows:

$$I_d = (1-D)\, I_L \tag{22}$$

6.4.2 Voltage source inverter

The three-phase three-level voltage source inverter proposed corresponds to a DC/AC switching power inverter using IGBTs operated through sinusoidal PWM (Molina & Mercado, 2006). The VSI structure proposed is designed to make use of a three-level twelve pulse pole structure, also called neutral point clamped (NPC), instead of a standard two-level six pulse inverter structure (Rodriguez et al., 2002, Soto & Green, 2002). This three-level VSI topology generates a more smoothly sinusoidal output voltage waveform than conventional two-level structures without increasing the switching frequency and effectively doubles the power rating of the VSI for a given semiconductor device. Moreover,

the three level pole attempts to address some limitations of the standard two-level by offering an additional flexibility of a level in the output voltage, which can be controlled in duration, either to vary the fundamental output voltage or to assist in the output waveform construction. This extra feature is used here to assist in the output waveform structure. In this way, the harmonic performance of the inverter is improved, also obtaining better efficiency and reliability. The output line voltage waveforms of a three-level VSI connected to a 380 V utility system are shown in Fig. 11. It is to be noted that in steady-state the VSI generates at its output terminals a switched line voltage waveform with high harmonics content, reaching the voltage total harmonic distortion (VTHD) almost 45% when unloaded. At the output terminals of the low pass sine wave filters proposed, the VTHD is reduced to as low as 1%, decreasing this quantity to even a half at the coupling transformer secondary output terminals (PCC). In this way, the quality of the voltage waveforms introduced by the PWM control to the power utility is improved and the requirements of IEEE Standard 519-1992 relative to power quality (VTHD limit in 5%) are entirely fulfilled (Bollen, 2000).

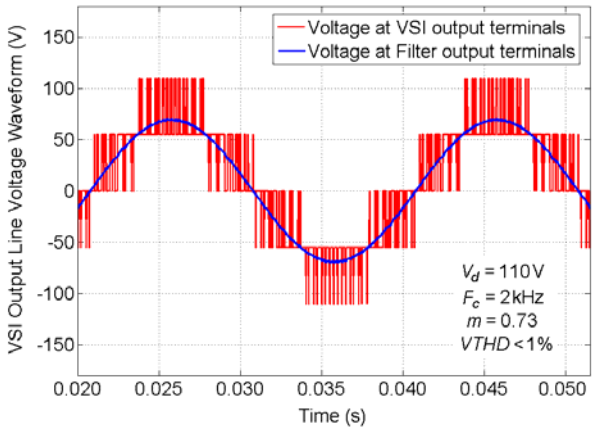

Fig. 11. Three-level NPC voltage source inverter output line voltage waveforms

The mathematical equations describing and representing the operation of the voltage source inverter can be derived from the detailed model shown in Fig. 10 by taking into account some assumptions respect to its operating conditions. For this purpose, a simplified equivalent VSI connected to the electric system is considered, also referred to as an averaged model, which assumes the inverter operation under balanced conditions as ideal, i.e. the voltage source inverter is seen as an ideal sinusoidal voltage source operating at fundamental frequency. This consideration is valid since, as shown in Fig. 11, the high-frequency harmonics produced by the inverter as result of the sinusoidal PWM control techniques are mostly filtered by the low pass sine wave filters and the net instantaneous output voltages at the point of common coupling resembles three sinusoidal waveforms phase-shifted 120º between each other.

This ideal inverter is shunt-connected to the network at the PCC through an equivalent inductance L_s, accounting for the leakage of the step-up coupling transformer and an equivalent series resistance R_s, representing the transformers winding resistance and VSI semiconductors conduction losses. The magnetizing inductance of the step-up transformer

can also be taken into consideration through a mutual equivalent inductance M. In the DC side, the equivalent capacitance of the two DC bus capacitors, C_{d1} and C_{d2} (C_{d1}=C_{d2}), is described through C_d=C_{d1}/2=C_{d2}/2 whereas the switching losses of the VSI and power losses in the DC capacitors are considered by a parallel resistance R_p. As a result, the dynamics equations governing the instantaneous values of the three-phase output voltages in the AC side of the VSI and the current exchanged with the utility grid can be directly derived by applying Kirchhoff's voltage law (KVL) as follows:

$$\begin{bmatrix} v_{inv_a} \\ v_{inv_b} \\ v_{inv_c} \end{bmatrix} - \begin{bmatrix} v_a \\ v_b \\ v_c \end{bmatrix} = \left(\mathrm{R_s} + s\mathrm{L_s}\right) \begin{bmatrix} i_a \\ i_b \\ i_c \end{bmatrix}, \tag{23}$$

where:

$$\mathrm{R_s} = \begin{bmatrix} R_s & 0 & 0 \\ 0 & R_s & 0 \\ 0 & 0 & R_s \end{bmatrix}, \qquad \mathrm{L_s} = \begin{bmatrix} L_s & M & M \\ M & L_s & M \\ M & M & L_s \end{bmatrix} \tag{24}$$

Under the assumption that the system has no zero sequence components (operation under balanced conditions), all currents and voltages can be uniquely transformed into the synchronous-rotating orthogonal two-axes reference frame, in which each vector is described by means of its d and q components, instead of its three a, b, c components. Thus, the new coordinate system is defined with the d-axis always coincident with the instantaneous voltage vector, as described in Fig. 12. By defining the d-axis to be always coincident with the instantaneous voltage vector v, yields v_d equals $|v|$, while v_q is null. Consequently, the d-axis current component contributes to the instantaneous active power and the q-axis current component represents the instantaneous reactive power. This operation permits to develop a simpler and more accurate dynamic model of the inverter.
By applying Park's transformation (Krause, 1992) stated by equation (25), equations (23) and (24) can be transformed into the synchronous rotating d-q reference frame as follows (equation (26)):

$$\mathrm{K_s} = \frac{2}{3} \begin{bmatrix} \cos\theta & \cos\left(\theta - \frac{2\pi}{3}\right) & \cos\left(\theta + \frac{2\pi}{3}\right) \\ -\sin\theta & -\sin\left(\theta - \frac{2\pi}{3}\right) & -\sin\left(\theta + \frac{2\pi}{3}\right) \\ \frac{1}{2} & \frac{1}{2} & \frac{1}{2} \end{bmatrix}, \tag{25}$$

with:

$\theta = \int_0^t \omega(\xi)d\xi + \theta(0)$: angle between the d-axis and the reference phase axis, and ξ: integration variable

ω: synchronous angular speed of the network voltage at the fundamental system frequency f (50 Hz throughout this chapter).

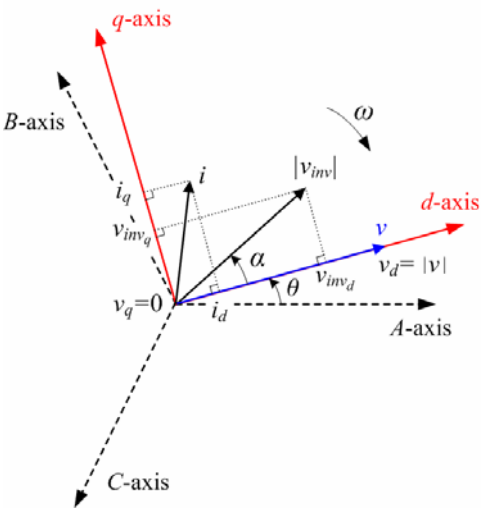

Fig. 12. Voltage source inverter vectors in the synchronous rotating *d-q* reference frame

Thus,

$$\begin{bmatrix} v_{inv_d} - v_d \\ v_{inv_q} - v_q \\ v_{inv_0} - v_0 \end{bmatrix} = \mathrm{K_s} \begin{bmatrix} v_{inv_a} - v_a \\ v_{inv_b} - v_b \\ v_{inv_c} - v_c \end{bmatrix}, \qquad \begin{bmatrix} i_d \\ i_q \\ i_0 \end{bmatrix} = \mathrm{K_s} \begin{bmatrix} i_a \\ i_b \\ i_c \end{bmatrix} \tag{26}$$

Then, by neglecting the zero sequence components, equations (27) and (28) are derived.

$$\begin{bmatrix} v_{inv_d} \\ v_{inv_q} \end{bmatrix} - \begin{bmatrix} v_d \\ v_q \end{bmatrix} = \left(\mathrm{R_s} + s\mathrm{L'_s}\right) \begin{bmatrix} i_d \\ i_q \end{bmatrix} + \begin{bmatrix} -\omega & 0 \\ 0 & \omega \end{bmatrix} \mathrm{L'_s} \begin{bmatrix} i_q \\ i_d \end{bmatrix}, \tag{27}$$

where:

$$\mathrm{R_s} = \begin{bmatrix} R_s & 0 \\ 0 & R_s \end{bmatrix}, \qquad \mathrm{L'_s} = \begin{bmatrix} L'_s & 0 \\ 0 & L'_s \end{bmatrix} = \begin{bmatrix} L_s - M & 0 \\ 0 & L_s - M \end{bmatrix} \tag{28}$$

It is to be noted that the coupling of phases *a-b-c* through the term *M* in matrix $\mathrm{L_s}$ (equation (24)), was fully eliminated in the *d-q* reference frame when the VSI transformers are magnetically symmetric, as is usually the case. This decoupling of phases in the synchronous-rotating system allows simplifying the control system design.

By rewriting equation (27), the following state equation can be obtained:

$$s \begin{bmatrix} i_d \\ i_q \end{bmatrix} = \begin{bmatrix} \dfrac{-R_s}{L'_s} & \omega \\ -\omega & \dfrac{-R_s}{L'_s} \end{bmatrix} \begin{bmatrix} i_d \\ i_q \end{bmatrix} + \frac{1}{L'_s} \begin{bmatrix} v_{inv_d} - |v| \\ v_{inv_q} \end{bmatrix} \tag{29}$$

A further major issue of the *d-q* transformation is its frequency dependence (ω). In this way, with appropriate synchronization to the network (through angle θ), the control variables in steady state are transformed into DC quantities. This feature is quite useful to develop an efficient decoupled control system of the two current components. Although the model is fundamental frequency-dependent, the instantaneous variables in the *d-q* reference frame contain all the information concerning the three-phase variables, including steady-state unbalance, harmonic waveform distortions and transient components.
The relation between the DC side voltage V_d and the generated AC voltage v_{inv} can be described through the average switching function matrix in the *d-q* reference frame $\mathbf{S_{av,dq}}$ of the proposed inverter, as given by equation (30). This relation assumes that the DC capacitors voltages are balanced and equal to $V_d/2$.

$$\begin{bmatrix} v_{inv_d} \\ v_{inv_q} \end{bmatrix} = \mathbf{S_{av,\,dq}}\, V_d\,, \tag{30}$$

and the average switching function matrix in *d-q* coordinates is computed as:

$$\mathbf{S_{av,\,dq}}=\begin{bmatrix} S_{av,d} \\ S_{av,q} \end{bmatrix} = \frac{1}{2} m_i\, a \begin{bmatrix} \cos\alpha \\ \sin\alpha \end{bmatrix}\,, \tag{31}$$

being,
m_i: modulation index of the voltage source inverter, $m_i \in [0, 1]$.
a: phase-shift of the inverter output voltage from the reference position,
$a = \frac{\sqrt{3}}{\sqrt{2}} \frac{n_2}{n_1}$: turns ratio of the step-up Δ–Y coupling transformer,
The AC power exchanged by the inverter is related to the DC bus power on an instantaneous basis in such a way that a power balance must exist between the input and the output of the inverter. In this way, the AC power should be equal to the sum of the DC resistance (R_p) power, representing losses (IGBTs switching and DC capacitors) and to the charging rate of the DC equivalent capacitor (C_d) (neglecting the wind generator action):

$$P_{AC} = P_{DC} \tag{32}$$

$$\frac{3}{2}\left(v_{inv_d} i_d + v_{inv_q} i_q\right) = -\frac{C_d}{2} V_d s V_d - \frac{V_d^2}{R_p} \tag{33}$$

Essentially, equations (23) through (33) can be summarized in the state-space as described by equation (34). This continuous state-space averaged mathematical model describes the steady-state dynamics of the ideal voltage source inverter in the *d-q* reference frame, and will be subsequently used as a basis for designing the middle level control scheme to be proposed. As reported by Acha et al. (2002), modelling of static inverters by using a synchronous-rotating orthogonal *d-q* reference frame offer higher accuracy than employing stationary coordinates. Moreover, this operation allows designing a simpler control system than using *a-b-c* or α-β.

$$s\begin{bmatrix} i_d \\ i_q \\ V_d \end{bmatrix} = \begin{bmatrix} \frac{-R_s}{L'_s} & \omega & \frac{S_{av,d}}{2L'_s} \\ -\omega & \frac{-R_s}{L'_s} & \frac{S_{av,q}}{2L'_s} \\ -\frac{3}{2C_d}S_{av,d} & -\frac{3}{2C_d}S_{av,q} & -\frac{2}{R_pC_d} \end{bmatrix} \begin{bmatrix} i_d \\ i_q \\ V_d \end{bmatrix} - \begin{bmatrix} \frac{|v|}{L'_s} \\ 0 \\ 0 \end{bmatrix} \tag{34}$$

7. Control strategy of the direct-driven PMSG wind turbine system

The proposed hierarchical three-level control scheme for the grid-connected direct-in-line wind turbine system is depicted in Fig. 13. This control system consists of three distinct blocks, namely the external, middle and internal level. Its design is based on concepts of instantaneous power on the synchronous-rotating *d-q* reference frame. This structure has the goal of rapidly and simultaneously controlling the active and reactive power provided by the wind turbine system (Molina & Mercado, 2009).

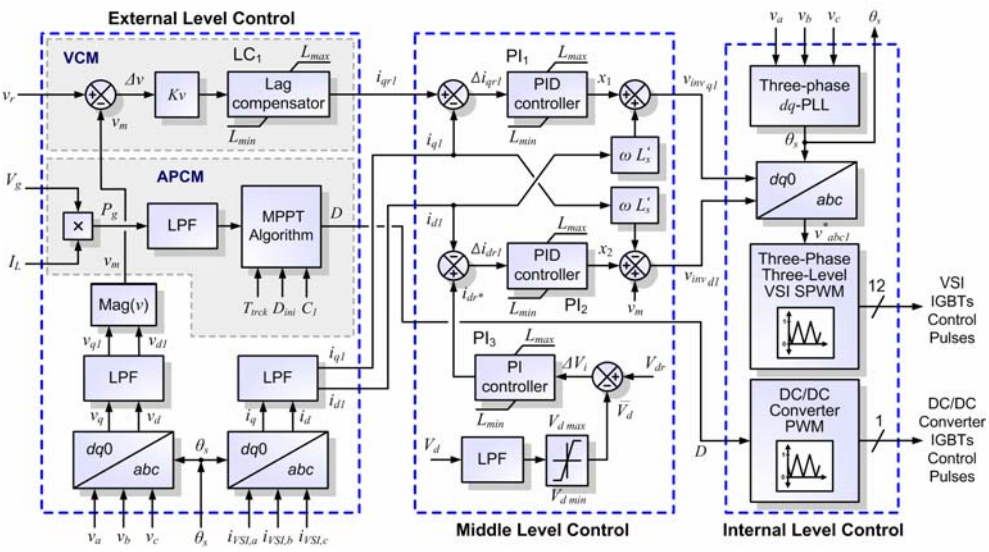

Fig. 13. Multi-level control scheme for the proposed three-phase grid-connected wind energy conversion system

7.1 External level control

The external level control, which is outlined in Fig. 13 (left side) in a simplified form, is responsible for determining the active and reactive power exchange between the WECS system and the utility grid. This control strategy is designed for performing two major control objectives: the voltage control mode (VCM) with only reactive power compensation capabilities and the active power control mode (APCM) for dynamic active power exchange with the AC network. To this aim, the instantaneous voltage at the PCC is computed by

employing a synchronous-rotating reference frame. In consequence, by applying Park's transformation, the instantaneous values of the three-phase AC bus voltages are transformed into *d-q* components, v_d and v_q respectively, and then filtered to extract the fundamental components, v_{d1} and v_{q1}. As formerly described, the *d-axis* was defined always coincident with the instantaneous voltage vector v, then v_{d1} results in steady-state equal to $|v|$ while v_{q1} is null. Consequently, the *d*-axis current component of the VSI contributes to the instantaneous active power p while the q-axis current component represents the instantaneous reactive power q, as stated in equations (35) and (36). Thus, to achieve a decoupled active and reactive power control, it is required to provide a decoupled control strategy for i_{d1} and i_{q1} (Timbus et al., 2009).

$$p = \frac{3}{2}(v_{d1}i_{d1} + v_{q1}i_{q1}) = \frac{3}{2}|v|\, i_{d1}\,, \tag{35}$$

$$q = \frac{3}{2}(v_{d1}i_{q1} - v_{q1}i_{d1}) = \frac{3}{2}|v|\, i_{q1}\,, \tag{36}$$

In this way, only v_d is used for computing the resultant current reference signals required for the desired SMES output active and reactive powers. Independent limiters are use for restrict both the power and current signals before setting the references i_{dr1} and i_{qr1}. Additionally, the instantaneous actual output currents of the wind turbine system, i_{d1} and i_{q1}, are computed for use in the middle level control. In all cases, the signals are filtered by using second-order low-pass filters to obtain the fundamental components employed by the control system.

The standard control loop of the external level is the VCM and consists in controlling (supporting and regulating) the voltage at the PCC through the modulation of the reactive component of the inverter output current, i_{q1}. This control mode has proved a very good performance in conventional reactive power static controllers. The design of this control loop in the rotating frame is simpler than using stationary frame techniques, and employs a standard proportional-integral (PI) compensator including an anti-windup system to enhance the dynamic performance of the VCM system. This control mode compares the reference voltage set by the operator with the actual measured value in order to eliminate the steady-state voltage offset via the PI compensator. A voltage regulation droop (typically 5%) R_d is included in order to allow the terminal voltage of the WTG to vary in proportion with the compensating reactive current. Thus, the PI controller with droop characteristics becomes a simple phase-lag compensator (LC_1), resulting in a stable fast response compensator. This feature is particularly significant in cases that more high-speed voltage compensators are operating in the area. This characteristic is comparable to the one included in generators´ voltage regulators.

The main purpose of a grid-connected wind turbine system is to transfer the maximum wind generator power into the electric system. In this way, the APCM aims at matching the active power to be injected into the electric grid with the maximum instant power generated by the wind turbine generator. This objective is fulfilled by using the output power signal P_g as an input for the maximum power point tracker (MPPT), which will be subsequently described. Maximum power point tracking means that the wind turbine is always supposed to be operated at maximum output voltage/current rating. From equations (3) and (4), the optimal rotational speed ω_{opt} of the wind turbine rotor for a given wind speed can be used to

obtain the maximum turbine efficiency $\eta_{t\max}$ and then the maximum mechanical output power of the turbine. Unfortunately, measuring the wind flowing in the wind turbine rotor is difficult and increases complexity and costs to the DG application, especially for small generating systems; so that to avoid using this measurement for determining the optimal rotor speed, an indirect approach can be implemented.

The wind turbine power is directly controlled by the DC/DC boost converter, while the generator speed in critical conditions is regulated by the pitch angle of the turbine blades. The pitch angle controller is only active in high wind speeds. In these circumstances, the rotor speed can no longer be controlled by increasing the generated power, as this would lead to overloading the generator and/or the converter. To prevent the rotor speed from becoming too high, which would result in mechanical damage, the blade pitch angle is changed in order to reduce the power coefficient C_p. At partial load, the pitch angle is kept constant to its optimal value, while the control of the electrical system via the chopper assures variable speed operation of the WTG.

The proposed MPPT strategy is based on directly adjusting the DC/DC converter duty cycle according to the result of the comparison of successive WTG output power measurements (Datta & Ranganathan, 2003). The control algorithm uses a "Perturbation and Observation" (P&O) iterative method that proves to be efficient in tracking the MPP of the WECS for a wide range of wind speeds. The algorithm, which was widely used for photovoltaic solar systems with good results (Molina et al., 2007), has a simple structure and requires few measured variables, as depicted in Fig. 14.

The WECS MPPT algorithm operates by constantly perturbing, i.e. increasing or decreasing, the rectified output voltage $V_g(k)$ of the WTG and thus controlling the rotational speed of the turbine rotor via the DC/DC boost converter duty cycle D and comparing the actual output power $P_g(k)$ with the previous perturbation sample $P_g(k-1)$. If the power is increasing, the perturbation will continue in the same direction in the following cycle so that the rotor speed will be increased, otherwise the perturbation direction will be inverted. This means that the WTG output voltage is perturbed every MPPT iteration cycle k at sample intervals T_{trck}. Therefore, when the optimal rotational speed of the rotor ω_{opt} for a specific wind speed is reached, the P&O algorithm will have tracked the MPP and then will settle at this point but with small oscillations. This allows driving the turbine automatically into the operating point with the highest aerodynamic efficiency and consequently leads to optimal energy capture using this controller. Above rated wind speed the pitch angle is increased to limit the absorbed aerodynamic power and the speed is controlled to its rated value ω_{lim}.

7.2 Middle level control

The middle level control makes the expected output, i.e. positive sequence components of i_d and i_q, to dynamically track the reference values set by the external level. The middle level control design, which is depicted in Fig. 13 (middle side), is based on a linearization of the state-space averaged model of the VSI in d-q coordinates, described in equation (34). Inspection of this equation shows a cross-coupling of both components of the inverter output current through ω. Therefore, in order to fully decouple the control of i_d and i_q, appropriate control signals have to be generated. To this aim, it is proposed the use of two control signals x_1 and x_2, which are derived from assumption of zero derivatives of currents ($s\, i_d$ and $s\, i_q$) in the upper part (AC side) of equation (34). This condition is assured by employing conventional PI controllers with proper feedback of the inverter actual output

current components, as shown in Fig. 13. Thus, i_d and i_q respond in steady-state to x_1 and x_2 respectively with no crosscoupling, as derived from equation (37). As can be noticed, with the introduction of these new variables this control approach allows to obtain a quite effective decoupled control with the VSI model (AC side) reduced to first-order functions.

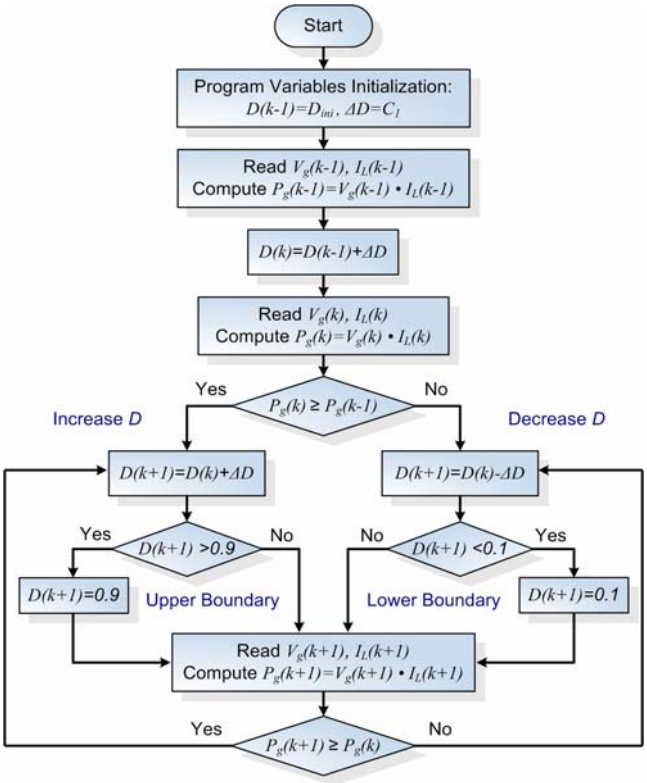

Fig. 14. Flowchart for the P&O MPPT algorithm

$$s\begin{bmatrix} i_d \\ i_q \end{bmatrix} = \begin{bmatrix} \dfrac{-R_s}{L'_s} & 0 \\ 0 & \dfrac{-R_s}{L'_s} \end{bmatrix} \begin{bmatrix} i_d \\ i_q \end{bmatrix} - \begin{bmatrix} x_1 \\ x_2 \end{bmatrix} \tag{37}$$

From equation (34), it can be seen the additional coupling resulting from the DC capacitors voltage V_d, as much in the DC side (lower part) as in the AC side (upper part). This difficulty demands to maintain the DC bus voltage as constant as possible, in order to decrease the influence of the dynamics of V_d. The solution to this problem is obtained by using another PI compensator which allows eliminating the steady-state voltage variations at the DC bus, by forcing the instantaneous balance of power between the DC and the AC sides of the inverter through the contribution of a corrective signal i_{dr^*}, and thus by the modulation of the duty cycle D of the DC/DC chopper.

7.3 Internal level control

The internal level provides dynamic control of input signals for the DC/DC and DC/AC converters. This level is responsible for generating the switching control signals for the twelve valves of the three-level VSI, according to the control mode (SPWM) and types of valves (IGBTs) used and for the single valve (IGBT) of the boost two-level DC/DC converter. Fig. 13 (right side) shows a basic scheme of the internal level control of the WTG unit. This level is mainly composed of a line synchronization module and a firing pulses generator for both the VSI and the chopper. A phase locked loop (PLL) is used for synchronizing through the phase θ_s, the pulses generated for the three-phase inverter. The phase signal is derived from the positive sequence components of the AC voltage vector measured at the PCC of the inverter. In the case of the sinusoidal PWM pulses generator block, the controller of the VSI generates pulses for the carrier-based three-phase PWM inverter using three-level topology. In the case of the DC/DC converter firing pulses generator block, the PWM modulator is built using a standard two-level PWM generator.

8. Digital simulation results

In order to investigate the effectiveness of the proposed models and control algorithms, digital simulations were performed using SimPowerSystems of MATLAB/Simulink (The MathWorks Inc., 2010). For validation of both control strategies, i.e. APCM and VCM of the wind power system, two sets of simulations were employed.

Simulations depicted in Fig. 15 show the case with only active power exchange with the utility grid, i.e. with just the APCM activated at all times, for the studied 0.5 kW WTG connected to a 380V/50Hz weak feeder. The incident wind flowing at the WTG rotor blades is forced to vary quickly in steps every 1s in the manner described in Fig. 15(a). This wind speed variation produces proportional changes in the maximum power that can be drawn from the WTG (MPP actual power shown in red dashed lines). As can also be observed in blue solid lines, the P&O maximum power tracking method proves to be accurate in following the MPP of the WTG with a settling time of almost 0.35s. The trade-off between fast MPP tracking and power error in selecting the appropriate size of the perturbation step can notably be optimized in efficiency. As can be noted in Fig. 15(b), all the active power generated by the WTG is injected into the electric grid trough the PCS, except losses, with small delays in the dynamic response (blue dashed lines). It can also be seen the case with fixed voltage control of the rectified voltage V_d, i.e. with no MPPT control and consequently with near constant rotor speed operation (green dotted lines). In this case, the power injected into the electric grid is much lesser than with MPPT, about up to 30% in some cases. Eventually, no reactive power is exchanged with the electric grid since the VCM is not activated (shown in red solid lines). In this way, as can be observed in Fig. 15(c), the instantaneous voltage at the point of coupling to the ac grid is maintained almost invariant at about 0.99 p.u. (per unit of 380 V base line-line voltage). It is also verified a very low transient coupling between the active and reactive (null in this case) powers exchanged by the grid-connected WTG due to the proposed full decoupled current control strategy in *d-q* coordinates.

Simulations of Fig. 16 show the case with both, active and reactive power exchange with the utility grid, i.e. the APCM is activated all the time while the VCM is activated at t=0.5 s. The WTG is now subjected to the same previous profile of wind speed variations, as described in Fig. 16(a). As can be seen, the maximum power for each wind speed condition is rapidly and

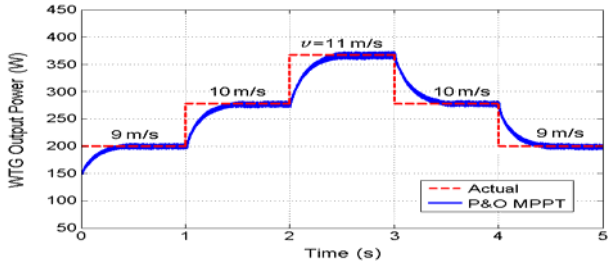

(a)

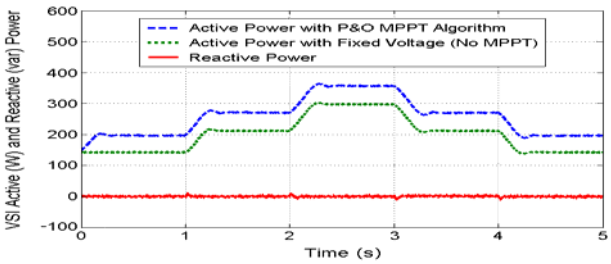

(b)

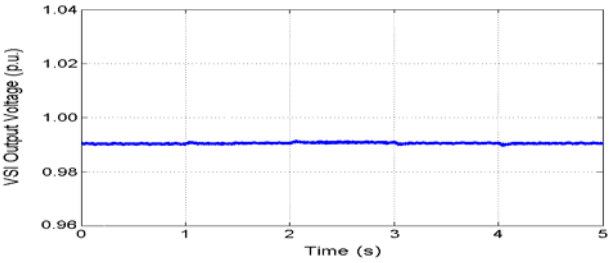

(c)

Fig. 15. Simulation results for active power exchange with the utility distribution grid (APCM). (a) PMSG generator output power. (b) VSI output active and reactive power. (c) PCC terminal voltage.

accurately drawn by the P&O MPPT method in the same way as in the previous case study, as depicted in blue solid lines in Fig. 16(b). This power is injected into the electric grid (blue dashed lines), except losses. These losses are increased with the injection of reactive power, causing a slightly lower exchange of active power than the previous case studied with both controls of the inverter (with and without MPPT). As shown in Fig. 16(c), the rapid injection of almost 320 var of reactive capacitive power into the electric utility system (red solid lines) when the VCM is activated aims at controlling the magnitude of the instantaneous voltage at the PCC around the reference voltage of 1 p.u. (or 380 V). Here it is also verified a very low transient coupling between the active and reactive powers injected into the AC grid due to the full decoupled current control strategy in the *d-q* reference frame.

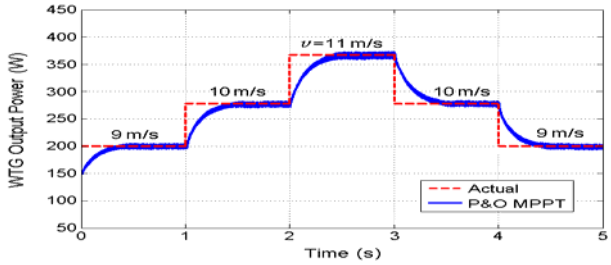

(a)

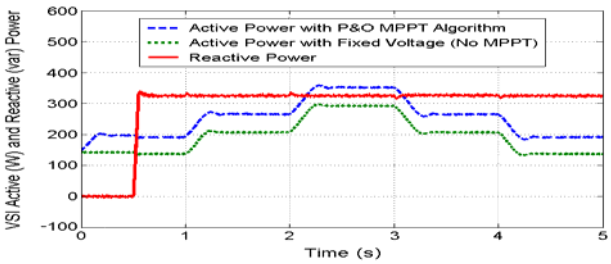

(b)

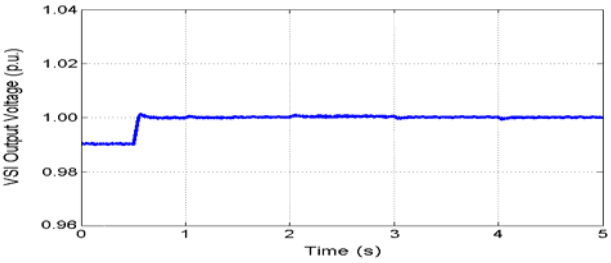

(c)

Fig. 16. Simulation results for simultaneous active and reactive power exchange with the utility distribution grid (APCM and VCM). (a) PMSG generator output power. (b) VSI output active and reactive power. (c) PCC terminal voltage.

9. Conclusion

This chapter has provided an overall perspective of modern wind power systems, including a discussion of major wind turbine concepts and technologies. More specifically, of the various wind turbine designs, pitch-controlled variable speed wind turbines controlled by means of power electronic converters have been considered. Among them, direct-in-line wind turbines with full-scale power converter and using direct-driven permanent magnet synchronous generators have increasingly drawn more interests to wind turbine manufactures due to its advantages over the other variable-speed wind turbines. Based on this issue, major operating characteristics of these devices have been thoroughly analyzed

and a three-phase grid-connected wind turbine system, incorporating a maximum power point tracker for dynamic active power generation has been presented. Moreover, a simplified state-space averaged mathematical model of the wind turbine system has been provided. An efficient power conditioning system of the selected wind turbine design and a new three-level control scheme by using concepts of instantaneous power in the synchronous-rotating *d-q* reference frame in order to simultaneously and independently control active and reactive power flow in the distribution network level have been proposed. Dynamic system simulation studies in the MATLAB/Simulink environment has been used in order to demonstrate the effectiveness of the proposed multi-level control approaches in *d-q* coordinates and the full detailed models presented. The fast response of power electronic devices and the enhanced performance of the proposed control techniques allow taking full advantage of the wind turbine generator.

10. Acknowledgments

The author wishes to thank CONICET (Argentinean National Research Council for Science and Technology), IEE/UNSJ (Institute of Electrical Energy at the National University of San Juan) and ANPCyT (National Agency for Scientific and Technological Promotion) under grant FONCYT PICT 2006 – Cod. No. 1790, for the financial support of this work.

11. References

Ackermann, T. (2005). *Wind Power in Power Systems*, John Wiley & Songs, 1st Ed., United Kingdom.

Acha, E.; Agelidis, V.; Anaya-Lara, O. & Miller, T. (2002). *Power Electronic Control in Electrical Systems,* Newness, 1st ed., United Kingdom.

Blaabjerg, F.; Chen, Z & Kjaer, S. B. (2004). Power Electronics as Efficient Interface in Dispersed Power Generation Systems. *IEEE Transactions on Power Electronics*, Vol. 19, No. 5, pp. 1184–1194.

Blaabjerg, F. & Chen, Z. (2006). *Power Electronics for Modern Wind Turbines,* Morgan & Claypool Publishers, 1st Ed., Seattle, WA, USA.

Bollen, M. H. J. (2000). *Understanding Power Quality Problems*. IEEE Press, Piscataway, New Jersey, USA.

Carrasco J. M.; Garcia-Franquelo, L.; Bialasiewicz, J. T.; Galván, E; Portillo-Guisado, R. C.; Martín-Prats, M. A.; León, J. I. & Moreno-Alfonso, N. (2006). Power Electronic Systems for the Grid Integration of Renewable Energy Sources: A Survey. *IEEE Trans. on Industrial Electronics*, Vol. 53, No. 4, pp. 1002-1016.

Chen, Z. & Blaabjerg, F. (2009). Wind Farm – A Power Source in Future Power Systems. *Renewable and Sustainable Energy Reviews*, Vol. 13, No. 6-7, pp. 1288–1300.

Datta R. & Ranganathan, V. T. (2003). A Method of Tracking the Peak Power Points for a Variable Speed Wind Energy Conversion System", *IEEE Transactions on Energy Conversion*, Vol.18, pp.163-168.

Freris, L. L. (1990). *Wind Energy Conversion Systems,* Prentice-Hall, 1st Ed., New Jersey, USA.

Global wind energy council (2006) Global Wind Energy Markets Continue to Boom – 2006 another record year, Available from http://www.gwec.net/ [June, 2007].

Guerrero, J. M.; Blaabjerg,F.; Zhelev, T.; Hemmes, K.; Monmasson, E.; Jemei, S.; Comech, M. P.; Granadino, R. & Frau, J. I. (2010). Distributed Generation: Toward a New Energy Paradigm. *IEEE Industrial Electronics Magazine*, Vol. 4, No. 1, pp. 52-64, March 2010.

Hansen, A. D.; Iov, F.; Blaabjerg, F. & Hansen L. H. (2004). Review of contemporary wind turbine concepts and their market penetration, Journal of Wind Engineering, Vol. 28, No. 3, pp. 247-263.

Heier, S. (2006). *Grid Integration of Wind Energy Conversion Systems*, John Wiley & Sons, 1st ed., United Kingdom.

Krause, P.C. (1992). *Analysis of Electric Machinery*, Mc Graw-Hill, New York, USA.

Krüger T. & Andresen, B. (2001) Vestas OptiSpeed - Advanced control strategy for variable speed wind turbines. *Proceedings of European Wind Energy Conference*, pp. 983-86, July 2-6, Copenhagen, Denmark.

Li, S.; Haskew, T. A.; Muljadi, E. & Serrentino, C. (2009). Characteristic Study of Vector-Controlled Direct-Driven Permanent Magnet Synchronous Generator In Wind Power Generation. *Electric Power Components and Systems*, Vol. 37, No. 10, pp. 1162-1179.

Mohan, N.; Undeland, T & Robbins, W. (1995). *Power Electronics: Converters, Applications and Design*, John Wiley & Sons, 1st Ed., New York.

Molina M. G. & Mercado P. E. (2006). Control Design and Simulation of DSTATCOM with Energy Storage for Power Quality Improvements, *Proceedings of IEEE/PES Transmission and Distribution Conference Latin America*, Caracas, Venezuela, Aug. 2006.

Molina M. G. & Mercado P. E. (2008). A New Control Strategy of Variable Speed Wind Turbine Generator for Three-Phase Grid-Connected Applications, *Proceedings of IEEE/PES Transmission and Distribution LA*, Bogotá, Colombia.

Molina M. G. & Mercado P. E. (2009). Control of Tie-Line Power Flow of Microgrid Including Wind Generation by DSTATCOM-SMES Controller. *Proceedings of IEEE Energy Conversion Congress and Exposition*, San José-CA, USA, Sept. 2009, pp. 2014-2021.

Molina, M. G.; Pontoriero, D. H. & Mercado, P. E. (2007). An Efficient Maximum-Power-Point-Tracking Controller for Grid-Connected Photo-Voltaic Energy Conversion System. *Brazilian Journal of Power Electronics*, Vol.12, No.2, pp. 147–154.

Muller, S.; Deicke, M. & De Doncker, R. W. (2002). Doubly Fed Induction Generator Systems for Wind Turbines. *IEEE Industry Applications Magazine*, Vol. 8, No. 3, pp. 26-33.

Qiao, W.; Harley, R. G. & Venayagamoorthy, G. K. (2007). Dynamic Modeling of Wind Farms With Fixed-Speed Wind Turbine Generators, *Proceedings of IEEE PES 2007 General Meeting*, June 24-8, Tampa, USA.

Raiambal, K. & Chellamuthu, C. (2002). Modeling and Simulation of Grid Connected Wind Electric Generating System, *Proc. IEEE TENCON*, pp.1847–1852.

Rahman, S. (2003). Going Green: The Growth of Renewable Energy, *IEEE Power and Energy Magazine*, Vol. 1, No. 6, pp. 16-18.

Rodríguez, J.; Lai, J. S. & Peng, F.Z. (2002). Multilevel Inverters: A Survey of Topologies, Controls, and Applications. *IEEE Transactions on Industrial Electronics*, Vol. 49, No. 4, pp. 724-738.

Soto, D. & Green, T. C. (2002). A Comparison of High-Power Converter Topologies for the Implementation of FACTS Controllers. *IEEE Trans. on Industrial Electronics*, Vol. 49, No. 5, pp. 1072-1080.

Slootweg J. G. & Kling, W. L. (2003). The Impact of Large Scale Wind Power Generation on Power System Oscillations, *Electric Power Systems Research*, Vol. 67, No. 1, pp. 9-20.

The MathWorks Inc. (2010). *SimPowerSystems for Use with Simulink: User's Guide*, R2010a, Available from http://www.mathworks.com [July, 2010].

Timbus, A.; Liserre, M.; Teodorescu, R.; Rodriguez, P. & Blaabjerg, F. (2009). Evaluation of Current Controllers For Distributed Power Generation Systems, IEEE Transactions on Power Electronics, Vol. 24, No. 3, pp. 654-664, March 2009.